

Accepted Manuscript

Catecholamines Facilitate Fuel Expenditure and Protect Against Obesity via a Novel Network of the Gut-Brain Axis in Transcription Factor *Skn-1*-deficient Mice

Shota Ushiyama, Yoshiro Ishimaru, Masataka Narukawa, Misako Yoshioka, Chisayo Kozuka, Naoki Watanabe, Makoto Tsunoda, Naomi Osakabe, Tomiko Asakura, Hiroaki Masuzaki, Keiko Abe



PII: S2352-3964(16)30174-8
DOI: doi: [10.1016/j.ebiom.2016.04.031](https://doi.org/10.1016/j.ebiom.2016.04.031)
Reference: EBIOM 584

To appear in: *EBioMedicine*

Please cite this article as: Ushiyama, Shota, Ishimaru, Yoshiro, Narukawa, Masataka, Yoshioka, Misako, Kozuka, Chisayo, Watanabe, Naoki, Tsunoda, Makoto, Osakabe, Naomi, Asakura, Tomiko, Masuzaki, Hiroaki, Abe, Keiko, Catecholamines Facilitate Fuel Expenditure and Protect Against Obesity via a Novel Network of the Gut-Brain Axis in Transcription Factor *Skn-1*-deficient Mice, *EBioMedicine* (2016), doi: [10.1016/j.ebiom.2016.04.031](https://doi.org/10.1016/j.ebiom.2016.04.031)

This is a PDF file of an unedited manuscript that has been accepted for publication. As a service to our customers we are providing this early version of the manuscript. The manuscript will undergo copyediting, typesetting, and review of the resulting proof before it is published in its final form. Please note that during the production process errors may be discovered which could affect the content, and all legal disclaimers that apply to the journal pertain.

Title:

Catecholamines facilitate fuel expenditure and protect against obesity via a novel network of the gut-brain axis in transcription factor *Skn-1*-deficient mice

Authors/Affiliations:

Shota Ushiyama^{1, #}, Yoshiro Ishimaru^{1, #}, Masataka Narukawa^{1, #}, Misako Yoshioka¹, Chisayo Kozuka², Naoki Watanabe³, Makoto Tsunoda⁴, Naomi Osakabe³, Tomiko Asakura¹, Hiroaki Masuzaki², Keiko Abe^{1, 5}

¹Department of Applied Biological Chemistry, Graduate School of Agricultural and Life Sciences, The University of Tokyo, 1-1-1 Yayoi, Bunkyo-ku, Tokyo 113-8657, Japan

²Division of Endocrinology, Diabetes and Metabolism, Hematology, Rheumatology (Second Department of Internal Medicine), Graduate School of Medicine, University of the Ryukyus, 207 Uehara, Nishihara, Okinawa 903-0215, Japan

³Department of Bio-science and Engineering, Shibaura Institute of Technology, 307 Fukasaku, Minuma-ku, Saitama 337-8570, Japan.

⁴Graduate School of Pharmaceutical Sciences, The University of Tokyo, 7-3-1 Hongo, Bunkyo-ku, Tokyo 113-0033, Japan

⁵Kanagawa Academy of Science and Technology, Takatsu-ku, Kawasaki-shi, Kanagawa, Japan

Contact:

Address: Department of Applied Biological Chemistry, Graduate School of Agricultural and Life Sciences, The University of Tokyo, 1-1-1 Yayoi, Bunkyo-ku, Tokyo 113-8657,

Japan;

Tel: +81-3-5841-1878, Fax: +81-3-5841-1879

E-mail: ayishi@mail.ecc.u-tokyo.ac.jp (Y.I.) and aka7308@mail.ecc.u-tokyo.ac.jp (K.A.)

Additional Footnotes: # These authors contributed equally to this work.

Key words:

energy metabolism, brush cells, catecholamine, insulin

Running title:

Effect of *Skn-1* gene deletion on energy homeostasis via the gut-brain axis

Abbreviations:

BAT, brown adipose tissue; ChgA, chromogranin A; CT, computed tomography; Dbh, dopamine- β -hydroxylase; Dclk1, doublecortin-like kinase 1; Ddc, dopa decarboxylase; GI, gastrointestinal; GIP, glucose-dependent insulinotropic peptide; GLP-1, glucagon-like peptide-1; GSIS, glucose-stimulated insulin secretion; HFD, high-fat diet; IPGTT, intraperitoneal glucose tolerance test; ITT, insulin tolerance test; KO, knockout; NEFA, non-esterified fatty acid; OGTT, oral glucose tolerance test; Pnmt, phenylethanolamine N-methyltransferase; RER, respiratory exchange ratio; SCC, solitary chemosensory cells; T3, triiodothyronine; T4, tetraiodothyronine; TG, triacylglycerol; Th, tyrosine hydroxylase; Trpm5, transient receptor potential melastatin 5; TSH, thyroid stimulating hormone; Ucp3, uncoupling proteins 3; WAT, white adipose tissue.

Highlights

Skn-1a is a crucial transcription factor for generating brush cells and type II taste cells in the gastrointestinal tract.

Despite unaltered food intake, *Skn-1* KO mice have reduced body weight with lower body fat due to elevated energy expenditure.

Urinary excretion of catecholamines was elevated in *Skn-1* KO mice, suggesting brain-mediated energy homeostatic pathways.

Research in context

Taste signals and nutrient stimuli sensed by the gastrointestinal tract are transmitted to the brain to regulate feeding behavior and energy homeostasis along the gut-brain axis. We propose the concept that taste-receiving cells in the oral cavity and/or food-borne chemicals-receiving brush cells in the gut are involved in regulation of the body weight and adiposity via the brain. The discovery of food-derived factors that regulate these cells may open new avenues for the treatment of obesity and diabetes.

Summary

Taste signals and nutrient stimuli sensed by the gastrointestinal tract are transmitted to the brain to regulate feeding behavior and energy homeostasis. This system is referred to as the gut-brain axis. Here we show that both brush cells and type II taste cells are eliminated in the gastrointestinal tract of transcription factor *Skn-1* knockout (KO) mice. Despite unaltered food intake, *Skn-1* KO mice have reduced body weight with lower body fat due to increased energy expenditure. In this model, 24-hr urinary excretion of catecholamines was significantly elevated, accompanied by increased fatty acid β -oxidation and fuel dissipation in skeletal muscle and impaired insulin secretion driven by glucose. These results suggest the existence of brain-mediated energy homeostatic pathways originating from brush cells and type II taste cells in the gastrointestinal tract and ending in peripheral tissues, including the adrenal glands. The discovery of food-derived factors that regulate these cells may open new avenues the treatment of obesity and diabetes.

Introduction

Taste signals and nutrient stimuli sensed by the gastrointestinal (GI) tract are transmitted to the central nervous system, including the nucleus of the solitary tract and hypothalamus, via afferent neurons and humoral mediators, thereby controlling feeding behavior and energy homeostasis. This system is referred to as the gut-brain axis (Cummings and Overduin, 2007; Furness, 2012). This information is subsequently conveyed from the brain to peripheral tissues via efferent sympathetic and parasympathetic nerves including preganglionic sympathetic splanchnic input to the adrenal glands. For example, gut incretins such as glucose-dependent insulintropic peptide (GIP) and glucagon-like peptide-1 (GLP-1), which are released from the intestinal enteroendocrine cells in response to nutrient ingestion, potentiate glucose-stimulated insulin secretion (GSIS) from pancreatic β -cells (Wu et al., 2015). GLP-1 also activates the GLP-1 receptors expressed on vagal afferent nerve terminals in the portal vein and in the brain across the blood-brain barrier, which is involved in the regulation of appetite (Katsurada et al., 2014; Kinzig et al., 2002; Vahl et al., 2007). Gavage of agonists for bitter taste receptor increases food intake via the secretion of ghrelin, a hormone that potentiates hunger sensation (Janssen et al., 2011).

The *Skn-1* (also known as *Pou2f3*) gene, which encodes the POU homeodomain transcription factor, was originally identified as a regulator of the differentiation of epidermal keratinocytes (Andersen et al., 1993; Andersen et al., 1997). We previously reported that *Skn-1a* is expressed in sweet, umami (savory), and bitter-sensing taste cells, which are referred to as type II taste cells (Matsumoto et al., 2011). Type II taste cells are completely eliminated in *Skn-1* knockout (KO) mice, resulting in loss of electrophysiological and behavioral responses to sweet, umami, and bitter tastes. Thus,

Skn-1a is critical for generating type II taste cells. *Skn-1a* is also required for the generation of *Trpm5*-expressing solitary chemosensory cells (SCCs) in the nasal respiratory epithelium and microvillous cells in the main olfactory epithelium (Ohmoto et al., 2013; Yamaguchi et al., 2014). *Skn-1a* is expressed in several tissues including the stomach, but not in the brain (Yukawa et al., 1993).

There are four major cell types in the small intestine: enterocytes and Goblet, Paneth, and enteroendocrine cells (van der Flier and Clevers, 2009). In addition to these cell types, brush cells (also referred to as tuft cells or caveolated cells) constitute a minor fraction (0.4%) of the adult mouse intestinal epithelium (Gerbe et al., 2012). Brush cells are supposed to be chemosensory cells (Young, 2011) and express transient receptor potential melastatin 5 (*Trpm5*), Doublecortin-like kinase 1 (*Dclk1*), and choline acetyltransferase (Bezencon et al., 2008; Gerbe et al., 2009; Gerbe et al., 2011; Saqui-Salces et al., 2011; Schütz B et al., 2015). The mechanisms of differentiation and the function of brush cells remain elusive.

In the present study, we found that *Skn-1a* regulates differentiation of *Trpm5*-expressing brush cells in the GI tract. *Skn-1* KO mice exhibited reduced body weight with lower body fat than wild-type (WT) littermates. Despite unaltered food intake, *Skn-1* KO mice exhibited increased energy expenditure, caused by augmented catecholamine secretion. Our work raises the concept that taste cells receiving sweet, bitter, and umami tastes as well as brush cells receiving food-borne chemicals are involved in regulating body weight and body fat. Collectively, the present study provides new insights into the regulation of energy homeostasis originating from brush cells and taste cells in the GI tract and signaling to peripheral tissues including the adrenal glands, via the brain.

Material and Methods

Experimental Animals

All animal experiments were approved by the Animal Care and Use Committee at The University of Tokyo. *Skn-1/Pou2f3*-deficient mice with a mixed 129 x C57BL/6J background were generated as previously described (Matsumoto et al., 2011) and then backcrossed to C57BL/6J for more than 10 generations. Male *Skn-1* KO mice and their WT littermates generated by crossing the heterozygous mice were used in the present study. Mice were fed a normal chow diet (Lab MR Breeder, Nosan Co., Yokohama, Japan) after weaning or High-Fat Diet 32 (CREA Japan Inc., Tokyo, Japan) from 4 weeks of age for more than 12 weeks to induce dietary obesity. Mice were maintained in a room with a constant temperature of $22\pm 1^{\circ}\text{C}$ under a 12-hr light-dark cycle (lights on at 8 a.m.). Tissue samples were collected from 12- to 16-week-old mice that were fasted for 18 hr.

X-ray Computed Tomography (CT) Scan Analysis

Mice older than 16 weeks were anesthetized using an isoflurane nebulizer (Muromachi Kikai Co. Ltd., Tokyo, Japan); a Latheta LCT-200 CT instrument (Aloka-Hitachi LCT-200, Tokyo, Japan) was then used to scan abdominal fat and muscle mass and extract thighbone density.

Blood Chemical Parameters

Blood was collected from approximately 20-week-old mice by cardiac puncture at 10 a.m. under ad libitum feeding condition and after 18-hr fasting. Serum chemical parameters and hormones (PTH, T3, and T4) were analyzed by Nagahama Life Science Laboratory (Shiga, Japan). Plasma insulin and leptin were measured using the Luminex 200™

System (Luminex, Austin, TX, USA) by GeneticLab Co., Ltd. (Sapporo, Japan). Plasma adiponectin and FGF21 were measured using mouse adiponectin ELISA (BioVender, Brno, Czech Republic) and mouse and rat FGF-21 ELISA (BioVender), respectively.

Indirect Calorimetry

Indirect calorimetry was performed on 20- to 28-week-old mice using an indirect calorimeter (ARCO-2000, Arco Systems Inc., Chiba, Japan) and spontaneous motor activity was measured using a pyroelectric infrared ray sensor (NS-AS01, Neuroscience Inc., Tokyo, Japan) for 3-4 days after 2 days of habituation essentially as described by Tschop et al. (Tschop et al., 2011) or with an indirect calorimeter (MK-5000RQ, Muromachi Kikai Co. Ltd.) as previously described (Watanabe et al., 2014). The respiratory exchange ratio (RER) was calculated as the molar ratio of V_{CO_2}/V_{O_2} . Energy expenditure (kcal per hour) was calculated as heat (kcal/h) = $(3.815 + 1.232 \times RER) \times V_{O_2}$.

Mitochondrial DNA Copy Number

To measure the mitochondrial DNA copy number, the ratio of mitochondrial DNA to genomic DNA was calculated by a previously described method (Watanabe et al., 2014). In brief, total DNA was extracted from the gastrocnemius of 14- to 19-week-old mice that were fasted for 16 hr using a QIAamp DNA mini kit (QIAGEN Ltd., Tokyo, Japan) and used for qPCR (Applied Biosystems Japan Ltd., Tokyo, Japan). We used the TaqMan Gene Expression Assay (Applied Biosystems Foster City, USA; ACTB, Mm00607939_s1; CYTB, Mm044225274). The PCR cycling conditions were 50°C for 2 min, 95°C for 10 min, and 40 cycles of 95°C for 15 s and 60°C for 1 min. The

mitochondrial DNA copy number is presented relative to nuclear DNA following amplification of the mitochondrial gene region (cytochrome *b* vs. the nuclear endogenous control region, β -actin).

DNA Microarray

DNA microarray analysis using total RNA extracted from the gastrocnemius of 12- to 16-week-old mice that were fasted for 18 hr was performed as previously described (Nakai et al., 2008) with minor modifications. In brief, Total RNA samples (100 ng each) were prepared and processed for microarray analysis using a 3' IVT Express kit and GeneChip® Mouse Genome 430 2.0 Array (Affymetrix, Santa Clara, CA, USA) according to the manufacturer's standard protocols. The raw microarray data (CEL files) were quantified by the Factor Analysis for Robust Microarray Summarization (FARMS) (Hochreiter et al., 2006) using the statistical language R (Team and Computing, 2005) and Bioconductor (Gentleman et al., 2004). To identify differentially expressed genes, the rank products (RP) method (Breitling et al., 2004) was applied to the FARMS-quantified data. All microarray data are MIAME compliant and have been deposited in a MIAME-compliant database, the National Center for Biotechnology Information (NCBI) Gene Expression Omnibus (<http://www.ncbi.nlm.nih.gov/geo/>, GEO Series accession number GSE76936), as described in more detail on the MGED Society web site (<http://www.mged.org/Workgroups/MIAME/miame.html>).

Fecal TG and Total Energy Content

Fecal lipids were extracted from dried feces of 15-week-old mice fed a HFD according to the Folch method (Folch et al., 1957), and the TG concentration was measured using the

Wako triglyceride E-Test (Wako Pure Chemical Industries, Ltd., Osaka, Japan). The total energy content of feces collected for 8 weeks was measured by bomb calorimetry.

Measurement of Urine Catecholamines

Twenty-four-hour urine (for catecholamine measurements) was collected into collection vials from 11- to 12-week-old mice individually housed in metabolic cages. To avoid spontaneous oxidation of catecholamine, 60 μ L of hydrochloric acid (6 mol/L) was added to the collection vials (Moreira-Rodrigues et al., 2012). The collected urine was purified using MonoSpin PBA (GL Sciences, Tokyo, Japan) and urine catecholamines were measured by HPLC as previously described (Tsunoda et al., 2011). In brief, Chromatography was performed using an Inertsil ODS-4 column (5 μ m, 250 x 20 mm i.d., GL Science) with acetate-citrate buffer at a flow rate of 0.5 mL/min and detected by electrochemical detection. The concentration of urine creatinine was measured using a LabAssay™ Creatinine kit (Wako Pure Chemical Industries, Ltd.).

qRT-PCR in Adrenal Glands

Total RNA was extracted from adrenal glands using RNeasy mini-columns (Qiagen, Venlo, Netherlands), followed by genomic DNA digestion using RNase-free DNase (Qiagen). First-strand cDNA was generated by reverse transcription from total RNA (Superscript III Reverse Transcription Kit; Life Technologies, Gaithersburg, MD). Levels of mRNA transcripts were determined by qPCR (ABI Prism 7000 Sequence Detection System, Applied Biosystems, Foster City, CA). cDNA levels were normalized against β -actin. PCR amplification was performed using TaqMan technology (TaqMan Gene Expression Assays, Applied Biosystems). The TaqMan probe IDs were as follows:

tyrosine hydroxylase (Th; Mm00447557_m1), dopa decarboxylase (Ddc; Mm00516688_m1), dopamine β -hydroxylase (Dbh; Mm00460472_m1), phenylethanolamine N-methyltransferase (Pnmt; Mm00476993_m1), and β -actin (Mm00607939_s1). The delta-delta method was used for relative quantification (Livak and Schmittgen, 2001).

OGTT, IPGTT, ITT, and Measurement of Insulin, GIP, and GLP-1

Gavage administration of glucose (3.0 mg/g of body weight for measurement of blood glucose, plasma insulin, and plasma total GIP; 5.0 mg/g of body weight for measurement of plasma active GLP-1; 2.0 mg/g of body weight for measurement of blood glucose and plasma insulin in mice fed a HFD) was performed on 16-week-old WT and *Skn-1* KO mice at 10 a.m. after 18-hr fasting (n=20-30 animals per group) using a syringe attached to a feeding needle (KN-349-M1, Natsume Seisakusho Co. Ltd., Tokyo, Japan) inserted through the mouth into the stomach. For IPGTT or ITT, mice were fasted for 18 or 4 hours, then injected intraperitoneally with glucose (1.5 mg/g of body weight) or insulin (0.75 mU/g of body weight), respectively. Tail blood samples were collected from the tail vein before gavage (time 0) and 15, 30, 45, 60, 90, and 120 min after gavage. For measurement of GIP and GLP-1, tail blood samples were collected into chilled tubes containing DPP-IV Inhibitor (Merck Millipore, Billerica, MA) and/or EDTA and aprotinin (for GLP-1; Wako Pure Chemical Industries, Ltd.) before gavage (time 0) and 15, 30, and 60 min after gavage (for GIP) or 10, 20, and 40 min after gavage (for GLP-1). Blood glucose, plasma insulin, plasma total GIP, and plasma active GLP-1 were measured by Glucose Pilot (Iwai Chemicals Co. Ltd., Tokyo, Japan), Ultra Sensitive Mouse Insulin ELISA Kit (Morinaga Institute of Biological Science Inc., Kanagawa, Japan), Rat/Mouse

GIP (Total) ELISA Kit (EZRMGIP-55K, Merck Millipore), and GLP-1 (Active) ELISA Kit (AKMGP-011, Shibayagi Co. Ltd., Gunma, Japan), respectively.

RT-PCR

First-strand cDNAs from 11 different tissues except the circumvallate papillae (Genostaff, Tokyo, Japan) were used for RT-PCR. For the circumvallate papillae, total RNA was extracted and reverse-transcribed into cDNA with an oligo dT primer. Approximately 500 bp of coding region encompassing multiple exons of Skn-1a was amplified from each cDNA for 30 cycles at an annealing temperature of 60°C. The volume of PCR products for Skn-1a loaded on the agarose gel was approximately normalized using the PCR product for GAPDH.

Islet Isolation and *In Vitro* Insulin Release from Mouse Islets

Isolated pancreatic islets were prepared by liberase (Roche Diagnostics, Basel, Switzerland) digestion, manually selected, and incubated in RPMI 1640 tissue culture medium (Life Technologies) supplemented with 10% (vol/vol) fetal bovine serum at 37°C overnight. Insulin secretion *in vitro* was measured in static incubations. Prior to experiments, islets were pre-incubated for 60 min at 37°C in Krebs-Ringer (KR) buffer composed of 119 mM NaCl, 4.7 mM KCl, 2.5 mM CaCl₂, 1.2 mM MgCl₂, 1.2 mM KH₂PO₄, 25 mM NaHCO₃, and 10 mM HEPES (pH 7.4) with 5% bovine serum albumin. The medium was gassed with 95% O₂ and 5% CO₂ to obtain constant pH and oxygenation. The groups of 10 islets were incubated for 60 min at 37°C in Krebs-Ringer buffer solution containing 2.5 mM glucose (low glucose). The islets were transferred to new low glucose Krebs-Ringer buffer and incubated for 60 min. Subsequently, the islets were incubated in

Krebs-Ringer buffer containing 25 mM glucose (high glucose) for 30 min. The supernatants from the second low-glucose solution and from the high-glucose solution were collected for the insulin ELISA assay and stored at -80°C. Insulin concentrations were measured using an Ultra Sensitive Mouse Insulin ELISA Kit (Morinaga Institute of Biological Science).

Immunohistochemistry

Rabbits were immunized with peptides corresponding to residues 1140-1153 (C+PASARDREYLESGL) of Trpm5 (Operon Biotechnologies, Tokyo, Japan). Preincubation of the antibody with peptide antigen (10 ng/ml) abolished the brush cell staining, confirming the specificity of the antibody (data not shown). The other primary antibodies used were as follows: rabbit anti-Skn-1a antibody (#sc-330, Santa Cruz Biotechnology, Santa Cruz, CA), rabbit anti-Dclk1 antibody (#AP7219b, Abgent, San Diego, CA), rabbit anti-ChgA antibody (#20085, ImmunoStar, Hudson, WI), and goat anti-GLP-1 antibody (#sc-7782, Santa Cruz Biotechnology). Immunohistochemistry was performed as previously described (Ishimaru et al., 2006). In brief, Fresh-frozen sections (10- μ m thick) were fixed in 4% paraformaldehyde (PFA), permeabilized with ice-cold methanol, blocked with phosphate-buffered saline (PBS) containing 5% skim milk, and incubated with rabbit anti-Skn-1a antibody (1/1,000 dilution), rabbit anti-Trpm5 antibody (1/200 dilution), rabbit anti-Dclk1 antibody (1/50 dilution), or rabbit anti-ChgA antibody (1/200 dilution), followed by incubation with Alexa Fluor 488- (#A21206) or Alexa Fluor 555-conjugated anti-rabbit IgG (#A31572, Life Technologies). For GLP-1, fresh-frozen sections (10- μ m thick) were fixed with 4% PFA, blocked with PBS containing 5% normal donkey serum and 0.2% Triton X-100, and incubated with goat anti-GLP-1 antibody

(1/150 dilution) followed by incubation with Alexa Fluor 555-conjugated anti-goat IgG (#A21432, Life Technologies).

For double staining, fresh-frozen sections (10- μ m thick) were fixed with 4% PFA and permeabilized with ice-cold methanol followed by antigen retrieval. The sections were then blocked with Tris-buffered saline with 0.05% Tween 20 (TBST) containing 5% skim milk and incubated with rabbit anti-Trpm5 antibody (1/200 dilution), followed by incubation with horseradish peroxidase (HRP)-conjugated anti-rabbit IgG (#31460, Life Technologies) and subsequent reaction with tyramide signal amplification (TSA)-Alexa Fluor 488 (Life Technologies) as a substrate for peroxidase. After antigen retrieval, the sections were blocked with TBST containing 5% skim milk and incubated with rabbit anti-Skn-1a antibody (1/300 dilution) or rabbit anti-Dclk1 antibody (1/50 dilution), followed by incubation with Cy3-conjugated anti-rabbit IgG (#711-165-152, Jackson ImmunoResearch, West Grove, PA).

In situ Hybridization

In situ hybridization was performed as previously described (Ishimaru et al., 2005). In brief, fresh-frozen sections (10- μ m thick) of the small intestine, including the duodenum, jejunum, and ileum, were placed on MAS-coated glass slides (Matsunami Glass, Osaka, Japan) and fixed in 4% PFA in PBS. Prehybridization (at 58°C for 1 hour), hybridization (at 58°C, 2 O/N), washing (0.2x SSC at 58°C), and development (NBT-BCIP) were performed using a digoxigenin-labeled probe for Trpm5. Stained images were obtained using a fluorescence microscope (BX51, Olympus, Tokyo, Japan) equipped with a cooled CCD digital camera (DP71, Olympus).

Data Analysis and Statistical Methods

All data are presented as the mean \pm SEM. Statistically significant differences were assessed using Student's *t*-test.

ACCEPTED MANUSCRIPT

Results

Brush cells in the GI tract are abolished in Skn-1 KO mice

We first investigated whether Skn-1a plays important roles in the regulation of cell differentiation in the stomach and small intestine. To examine the mRNA expression of *Skn-1a* in the GI tract, we performed RT-PCR analysis of mRNA from several tissues of WT mice. *Skn-1a* was abundantly expressed in the circumvallate papillae, stomach, duodenum, jejunum, and ileum, but it was absent or only faintly expressed in all other tissues examined, including the pancreas, islets of Langerhans, brain, liver, skeletal muscle, white adipose tissue (WAT), and brown adipose tissue (BAT) (Fig. 1a). RT-PCR of GAPDH as a control revealed comparable levels in all the tissues other than islets of Langerhans and WAT, in which slightly less intense bands were detected (Fig. 1a). To examine the tissue distribution of *Skn-1a* in the stomach and intestine at the cellular level, we next performed immunohistochemistry using an anti-Skn-1a antibody. In the stomach, Skn-1a signals were abundantly detected in the corpus beneath the limiting ridge (Fig. 1b). In the duodenum, jejunum, and ileum, Skn-1a signals were observed in approximately 100 cells per section (Fig. 1b and data not shown). These results suggest that Skn-1a functions as a transcription factor that regulates cell differentiation in the stomach and intestine as well as in the taste buds, nasal respiratory epithelium, and main olfactory epithelium (Matsumoto et al., 2011; Ohmoto et al., 2013; Yamaguchi et al., 2014).

We next examined the expression of *Trpm5* in the small intestine. *In situ* hybridization analysis using a probe for *Trpm5* revealed that *Trpm5* signals scattered throughout the small intestine including the duodenum, jejunum, and ileum, of WT mice (Fig. 1c and data not shown), consistent with the previous reports (Bezencon et al., 2008). Intriguingly,

no signals of *Trpm5* were observed in *Skn-1* KO mice (Fig. 1c). Immunohistochemistry using an anti-*Trpm5* antibody confirmed the presence of the *Trpm5* protein in the duodenum of WT mice but the absence of *Trpm5* protein in *Skn-1* KO mice (Fig. S1a).

Doublecortin-like kinase 1 (*Dclk1*) antibody marks brush cells (Gerbe et al., 2009; Gerbe et al., 2011; Saqui-Salces et al., 2011). Chromogranin A (*ChgA*) is a marker for enteroendocrine cells (Rindi et al., 2004). GLP-1 is an incretin, a peptide hormone, secreted from enteroendocrine L cells (Wu et al., 2015). Signals of *Dclk1* were detected in WT mice but not in *Skn-1* KO mice (Fig. 1d). By contrast, signals of *ChgA* and GLP-1 were observed in WT and *Skn-1* KO mice (Fig. S1a). Finally, we performed double staining using antibodies against *Trpm5* and *Skn-1a* or *Dclk1*. Nearly all *Trpm5*-positive cells were also positive for *Skn-1a* or *Dclk1* (Figs. 1e and S1b). Taken together, these results demonstrate that brush cells expressing *Trpm5* and *Dclk1* are abolished in *Skn-1* KO mice and that *Skn-1a* is a crucial transcription factor for generating brush cells in the GI tract.

Metabolic phenotypes of Skn-1 KO mice fed a normal chow diet

To examine the effect of eliminating type II taste cells and brush cells in the GI tract on energy homeostasis, we characterized the metabolic phenotypes of *Skn-1* KO mice. Whereas there was no significant difference in body weight at birth between the *Skn-1* KO and WT littermates (Fig. S2a), *Skn-1* KO mice exhibited lower body weight compared to their WT littermates when weaned at 3 weeks of age (Figs. 2a and S2a). When fed a normal chow diet, *Skn-1* KO mice exhibited significantly lower body weight than their WT littermates throughout the 13 weeks after weaning (Fig. 2a). For example, the body weights of the *Skn-1* KO and WT littermates at 16 weeks of age were 27.4 ± 0.5 g and

29.8 ± 0.4 g, respectively. X-ray computed tomography (CT) analysis of body composition revealed that *Skn-1* KO mice had a lower body fat percentage than their WT littermates at approximately 20 weeks of age, whereas there was no significant difference in muscle mass percentage between the two genotypes (Fig. 2b). Among blood chemical parameters, the concentration of serum total ketone bodies was significantly higher in *Skn-1* KO mice than in their WT littermates under ad libitum feeding and 18-hr fasting conditions (Figs. 2c and 2d). In addition, some parameters related to lipid metabolism, such as cholesterol and non-esterified fatty acid (NEFA) levels, tended to be higher in *Skn-1* KO mice compared with their WT littermates (Tables S1 and S2). Collectively, these results demonstrate that lipid metabolism, such as lipid degradation and β -oxidation of fatty acids, is accelerated in *Skn-1* KO mice.

Despite the lower body weight and body fat percentage of *Skn-1* KO mice, there was no difference in food intake between the *Skn-1* KO and WT littermates at 8 weeks of age (Fig. 2e) and in water intake between the two genotypes (data not shown). Analysis of the metabolic rates of the mice revealed that the energy expenditure of *Skn-1* KO mice was higher than that of their WT littermates (Fig. 2f). By contrast, there were no significant differences in the respiratory exchange ratio (RER) or spontaneous motor activity between the two genotypes (Figs. S2b and S2c). These results demonstrate that increased energy expenditure causes reduced body weight with lower body fat percentage in *Skn-1* KO mice.

Quantitative real-time PCR (qPCR) analysis revealed that the mitochondrial DNA content in the skeletal muscle was significantly higher in *Skn-1* KO mice than in their WT littermates (Fig. 2g). Moreover, DNA microarray analysis revealed enhanced expression of genes involved in mitochondrial function, such as uncoupling proteins 3 (Ucp3), in

Skn-1 KO mice (Table 1). These results suggest that energy expenditure is increased in the skeletal muscle of *Skn-1* KO mice.

Metabolic phenotypes of Skn-1 KO mice fed a HFD

We next examined the metabolic phenotypes of *Skn-1* KO mice fed a HFD. When fed a HFD for more than 12 weeks after 4 weeks of age, the body weight of *Skn-1* KO mice was dramatically lower than that of their WT littermates (Fig. 3a). For example, the body weights of *Skn-1* KO and WT littermates at 16 weeks of age were 30.4 ± 0.9 g and 39.5 ± 0.9 g, respectively. CT analysis of body composition and measurement of tissue mass revealed that *Skn-1* KO mice had a lower body fat percentage, including epididymal and perirenal white adipose tissues, than their WT littermates at approximately 20 weeks of age, whereas there were no significant differences in the weight ratios of other tissues, such as muscle, between the two genotypes (Figs. 3b and 3c and Table S3).

Although there was no significant difference in food intake between the *Skn-1* KO and WT littermates at 8 weeks of age (Fig. 3d), energy expenditure was higher in *Skn-1* KO mice than in their WT littermates, but spontaneous motor activity was similar between the two genotypes (Fig. 3e and data not shown). In addition, we observed no differences in food intake or fecal triacylglycerol (TG) between the *Skn-1* KO and WT littermates at 15 weeks of age (Figs. S3a and S3b). Fecal energy content was also comparable between the *Skn-1* KO and WT littermates (Fig. S3c). These results suggest that increased energy expenditure is the primary cause of reduced adiposity in *Skn-1* KO mice fed a HFD.

Finally, we measured plasma adiponectin, FGF21, insulin, and leptin in *Skn-1* KO and WT littermates fed a HFD (Table S4). Plasma leptin tended to be lower in *Skn-1* KO mice

compared with their WT littermates ($p=0.08$).

Catecholamine secretion is augmented in Skn-1 KO mice fed a HFD

We examined whether the levels of thyroid hormones, including triiodothyronine (T3), tetraiodothyronine (T4), and thyroid stimulating hormone (TSH), and catecholamines, including norepinephrine, epinephrine, and dopamine, were altered in *Skn-1* KO mice fed a HFD. Serum T3, T4, and TSH were comparable between *Skn-1* KO and WT littermates (Fig. 4a). We next measured 24-hr urinary excretion of catecholamines. Urinary epinephrine and dopamine were significantly higher and norepinephrine tended to be higher ($p=0.06$) in *Skn-1* KO mice compared to their WT littermates (Fig. 4b). qPCR analysis revealed that the gene expression of catecholamine biosynthetic enzymes, including tyrosine hydroxylase (Th), dopa decarboxylase (Ddc), dopamine- β -hydroxylase (Dbh), and phenylethanolamine N-methyltransferase (Pnmt), in adrenal glands was comparable between *Skn-1* KO and their WT littermates (Fig. S4). These results suggest that catecholamines are over-secreted from adrenal glands in *Skn-1* KO mice.

Insulin secretion is reduced in Skn-1 KO mice

To examine carbohydrate metabolism in *Skn-1* KO mice, we performed an oral glucose tolerance test (OGTT). Blood glucose concentrations in *Skn-1* KO and WT littermates were comparable for 120 min after oral glucose administration (Fig. 5a). By contrast, the increase in plasma insulin 60 min after glucose administration was smaller in *Skn-1* KO mice than in their WT littermates (Fig. 5b). However, plasma GIP and GLP-1, which potentiate insulin secretion from pancreatic β -cells (Wu et al., 2015), were

comparable between *Skn-1* KO and WT littermates after oral glucose administration (Figs. S5a and S5b).

We next examined the insulin secretion ability of pancreatic β -cells in *Skn-1* KO mice. First, RT-PCR analysis revealed that *Skn-1a* was not expressed in the pancreas or islets of Langerhans of WT mice (Fig. 1a). Second, insulin secretion from isolated islets in response to 25 mM glucose was comparable between *Skn-1* KO and WT littermates (Fig. S5c). Third, in the intraperitoneal glucose tolerance test (IPGTT), blood glucose concentrations were comparable between *Skn-1* KO and WT littermates for 120 min after administration (Fig. S5d). Plasma insulin concentrations were also comparable between *Skn-1* KO and WT littermates before and at 15 min after intraperitoneal administration (Fig. S5e). Collectively, these results demonstrate that insulin secretion from pancreatic β -cells is normal in *Skn-1* KO mice. Finally, the insulin tolerance test (ITT) revealed that *Skn-1* KO and WT littermates had comparable insulin sensitivity (Fig. S5f).

When fed a HFD, blood glucose was significantly lower in *Skn-1* KO mice than their WT littermates for 120 min after oral glucose administration (Fig. 5c), demonstrating that impaired glucose tolerance in WT littermates fed a HFD is improved in *Skn-1* KO mice. In addition, plasma insulin levels were lower in *Skn-1* KO mice than in their WT littermates before glucose administration ($p < 0.05$) and tended to be lower at 15 min after administration ($p = 0.10$, Fig. 5d). ITT revealed that the *Skn-1* KO mice had improved insulin resistance compared with their WT littermates (Fig. 5e). Collectively, these results demonstrate that the insulin resistance and impaired glucose tolerance observed in WT mice fed a HFD are ameliorated in *Skn-1* KO mice.

Discussion

In the present study, we demonstrated that brush cells and type II taste cells in the GI tract (Matsumoto et al., 2011) are unexpectedly abolished in *Skn-1* KO mice. This finding indicates that *Skn-1* is critical for the development of *Trpm5*-expressing chemosensory cells in mice. The *Skn-1* KO mice had reduced body weight with a lower body fat percentage, primarily due to increased energy expenditure. Furthermore, catecholamine secretion was increased in *Skn-1* KO, accompanied by decreased insulin secretion. We propose brain-mediated mechanisms of energy homeostasis originating from brush cells and taste cells in the GI tract to peripheral tissues including the adrenal glands (Fig. 6). In detail, taste signals and nutrient stimuli, which are sensed by taste cells and brush cells in the GI tract are transmitted to the brain via afferent neurons and/or humoral mediators and subsequently conveyed to adrenal glands that secrete catecholamines via efferent sympathetic nerves. In *Skn-1* KO mice, loss of taste and/or nutrient sensing may intensify the activity of the efferent sympathetic nerves, resulting in exaggerated secretion of catecholamines. Based on the network of the gut-brain axis originating from brush cells and taste cells in the GI tract, the present study suggests an approach to the treatment of obesity.

Skn-1a is expressed in *Trpm5*-expressing chemosensory cells. Loss-of-function of *Skn-1a* results in the elimination of these cell types (Matsumoto et al., 2011; Ohmoto et al., 2013; Yamaguchi et al., 2014). In the present study, we demonstrated that *Skn-1a* is expressed in *Trpm5*-expressing brush cells in the GI tract including stomach and intestine. It should be noted that these cells are abolished in the GI tract of *Skn-1* KO mice. Genes encoding sweet taste receptors (T1R2 and T1R3) and downstream signaling molecules such as gustducin are expressed in enteroendocrine L cells that secrete GLP-1

(Jang et al., 2007). When glucose was orally administered, the plasma GLP-1 concentration was not augmented in *gustducin* KO mice compared with WT mice, which resulted in a lack of a rapid increase in plasma insulin levels and an impaired glucose tolerance (Jang et al., 2007). We showed that GLP-1 signals were similar between WT and *Skn-1* KO mice in immunohistochemical analyses, consistent with normal incretin release after oral glucose administration in *Skn-1* KO mice. These results demonstrate that *Skn-1a* is also required for the generation of *Trpm5*-expressing brush cells, but not for enteroendocrine L cells, in the GI tract.

Trpm5 is expressed not only in the chemosensory cells but also in the mouse pancreatic β -cell line MIN6, pancreatic islets of Langerhans, and pancreatic β -cells (Colsoul et al., 2010; Nakagawa et al., 2009; Oya et al., 2011; Prawitt et al., 2003; Yamamoto and Ishimaru, 2013). *Trpm5* plays an important role in the regulation of GSIS from pancreatic β -cells via two major mechanisms: triggering and amplifying pathways (Brixel et al., 2010; Colsoul et al., 2010; Liman, 2010). *Trpm5* KO mice, like *Skn-1* KO mice, gain significantly less body weight and fat mass and are more sensitive to insulin than WT mice when fed either a HFD or a high-carbohydrate diet (Larsson et al., 2015). *T1R3* is the common subunit of sweet (*T1R2+T1R3*) and umami (*T1R1+T1R3*) taste receptors (Yarmolinsky et al., 2009). When fed a HFD, *T1R3* KO mice had reduced fat mass, in spite of unaltered body weight (Simon et al., 2014). *T1R3* is expressed in the gut, pancreas, and adipose tissue as well as in the tongue (Yamamoto and Ishimaru, 2013). In contrast, *Skn-1a* was not expressed in the pancreas, islets of Langerhans, or brain, suggesting that the tissue distribution of *Skn-1a* is more restricted than that of *Trpm5* and *T1R3*. In this context, *Skn-1* KO mice are unique models for investigating unexplored mechanisms underlying the gut-brain axis and whole-body energy

metabolism.

Skn-1 KO mice exhibited lower body weight than their WT littermates after weaning when fed either a normal chow diet or a HFD, whereas body weight was indistinguishable between *Skn-1* KO and WT littermates at birth. Notably, the *Skn-1* KO mice had much lower body weight than their WT littermates when fed a HFD; the body weight gain of *Skn-1* KO mice fed a HFD for 12 weeks was nearly equivalent to that of WT mice fed a chow diet during the same period, and the *Skn-1* KO mice did not become obese. In *Skn-1* KO mice fed a HFD, blood glucose levels and insulin secretion as well as insulin tolerance were improved, and plasma leptin, an indicator of body fat mass, tended to be lower than in their WT littermates. These results demonstrate that *Skn-1* KO mice are resistant to HFD-induced metabolic dysregulation.

The reduced body weight of *Skn-1* KO mice was not due to decreased food intake or nutrient absorption but to increased energy consumption, which resulted in a lower body fat ratio. *Skn-1* KO mice exhibited slightly but significantly higher urinary epinephrine and dopamine, implying an increase in the total amounts of these hormones released in 24 hours. Because there was no difference in the expression of the biosynthetic enzymes for catecholamine in the adrenal glands, it is unlikely that this significant increase in catecholamine excretion was caused by catecholamine overproduction. Because peripheral secretion of catecholamine is induced by activation of the sympathetic nervous system (Watanabe et al., 1988) and *Skn-1a* is not expressed in the brain, it is tempting to speculate that the sympathetic nervous system in *Skn-1* KO mice is activated by unidentified signals from the GI tract to the brain and not alteration of brain function.

In particular, epinephrine and norepinephrine are critical to maintain energy production under hypoglycemia and malnutrition through lipolysis, ketogenesis (Bahnsen et al.,

1984; Steiner et al., 1991), and increased mitochondria in skeletal muscle (Miura et al., 2007). In adipocytes, catecholamines induce lipolysis, but insulin inhibits lipolysis (Nielsen et al., 2014). Consistent with previous reports, the copy number of mitochondrial DNA and the concentration of serum total ketone bodies were increased in *Skn-1* KO mice, in accordance with an increase in energy consumption in this model. These results indicate that the appropriate elevation of catecholamine secretion in *Skn-1* KO mice may protect against obesity and metabolic syndrome. Acute psychosocial stress induces changes in catecholamine sensitivity (Strahler et al., 2015). Pheochromocytoma is a tumor arising from adrenomedullary chromaffin cells that automatically overproduce catecholamines (Lenders et al., 2014). Patients with pheochromocytoma with similar levels of circulating catecholamines exhibit variable phenotypes, possibly due in part to differences in hormone sensitivity to the corresponding receptors (Markou et al., 2015). Catecholamine sensitivity in peripheral tissues may be similarly enhanced by stress signals from the brain in *Skn-1* KO mice.

In the OGTT, *Skn-1* KO mice exhibited a smaller increase in plasma insulin compared with their WT littermates, whereas blood glucose concentrations were indistinguishable between *Skn-1* KO and WT littermates. Why did the *Skn-1* KO mice exhibit such a reduced increase in plasma insulin despite similar changes in blood glucose? First, plasma concentrations of incretins, such as GIP and GLP-1, were comparable between *Skn-1* KO and WT littermates after oral glucose administration, which is consistent with the immunohistochemical analyses revealing that GLP-1 signals were similar between WT and *Skn-1* KO mice. Second, insulin secretion from pancreatic β -cells was normal in *Skn-1* KO mice. Third, *Skn-1* KO and WT littermates showed comparable insulin sensitivity in the ITT. By contrast, urinary epinephrine and dopamine were significantly

higher in *Skn-1* KO mice than their WT littermates. Catecholamines inhibit insulin secretion from pancreatic β -cells (Barth et al., 2007). Overexpression of pancreatic alpha2A-adrenergic receptor in the diabetic Goto-Kakizaki rat mediates adrenergic suppression of insulin secretion (Rosengren et al., 2009). Higher catecholamine secretion may inhibit insulin secretion in *Skn-1* KO mice. Collectively, our results demonstrate that enhanced catecholamine secretion in *Skn-1* KO mice induces lipolysis in WAT, accelerates β -oxidation of fatty acids in the liver and skeletal muscle, and, consequently, thermogenesis in skeletal muscle, and inhibits insulin secretion from the pancreas. A range of diverse effects contribute to resistance to HFD-induced obesity and fuel dyshomeostasis (Fig. 6). Further studies are warranted to elucidate the molecular mechanisms underlying the regulation of energy metabolism originating from brush cells and type II taste cells in the GI tract, e.g., identifying which chemosensory receptors are expressed in the brush cells of the GI tract.

Conclusions

In a network of the gut-brain axis, the loss of brush cells and taste cells in the GI tract alters energy metabolism in *Skn-1* KO mice. We thus propose the concept that taste-receiving cells in the oral cavity and/or food-borne chemicals-receiving brush cells in the gut are involved in regulation of the body weight and adiposity. The discovery of food-derived factors that regulate these cells may open new avenues for the treatment of obesity and diabetes.

Conflicts of Interest

The authors declare that they have no conflicts of interest.

Author Contributions

S.U., Y.I., and K.A. designed the experiments. S.U., Y.I., M.N., M.Y., and N.W. performed experiments and analyzed the data. C.K. and M.T. guided the experimental methods. N.O., T.A., and H.M. participated in discussions. S.U., Y.I., M.N., H.M., and K.A. wrote the paper.

Acknowledgments

We are grateful to Ms. Taeko Fukuda, Haruka Fujihira, and Rieko Imabayahsi for excellent technical assistance. We thank Dr. Ichiro Matsumoto and Dr. Makoto Ohmoto for backcrossing *Skn-1*-deficient mice to C57BL/6J mice. This work was supported in part by a Grant-in-Aid for Scientific Research (B) 25292068 to Y.I.; Grant-in-Aid for challenging Exploratory Research 25560046 to K.A. from the Ministry of Education, Culture, Sports, Science, and Technology of Japan; and the Council for Science, Technology and Innovation (CSTI) Cross-ministerial Strategic Innovation Promotion Program (SIP), “Technologies for creating next-generation agriculture, forestry and fisheries.”

Figure Legends**Fig. 1.** Brush Cells Are Eliminated in the GI Tract of *Skn-1* KO Mice

(a) Tissue distribution of *Skn-1a*. RT-PCR analysis revealed that *Skn-1a* was abundantly expressed in the circumvallate papillae, stomach, duodenum, jejunum, and ileum but absent or only faintly expressed in all other tissues examined, including the pancreas, islets of Langerhans, brain, liver, skeletal muscle, white adipose tissue (WAT), and brown adipose tissue (BAT).

(b) Immunostaining revealed strong *Skn-1a* signals in the corpus beneath the limiting ridge in the stomach (upper panel) and in a subset of cells in the small intestine (lower panel). Inset in the upper right corner of each panel shows higher magnification image of the area enclosed by the dashed box.

(c) *In situ* hybridization revealed that *Trpm5* mRNA was expressed in the jejunum of WT mice (upper panel) but not in *Skn-1* KO mice (lower panel).

(d) Immunostaining revealed *Dclk1* signals in WT mice (upper panel) but not *Skn-1* KO mice (lower panel). The arrowheads indicate signals.

(e) Double immunostaining demonstrated that nearly all *Trpm5*-positive cells were also positive for *Skn-1a*. The arrows indicate cells expressing *Trpm5* and *Skn-1a*. Scale bars: 100 μm and 25 μm (Inset). See also Fig. S1.

Fig. 2. Metabolic Phenotypes of *Skn-1* KO Mice Fed a Normal Chow Diet

(a) Changes in body weight under normal chow diet conditions. When fed a normal chow diet, *Skn-1* KO mice had lower body weight than their WT littermates for 13 weeks after weaning ($n > 75$). Also see Fig. S2A.

(b) *Skn-1* KO mice had a lower body fat percentage than their WT littermates, whereas

there was no significant difference in muscle mass percentage between the two genotypes (n=10-19).

(c and d) Serum levels of total ketone bodies were higher in *Skn-1* KO mice than their WT littermates under ad libitum feeding (n=18-28) (c) and 18-hr fasting conditions (n=13) (d).

(e) *Skn-1* KO and WT littermates had similar food intake at 8 weeks of age (n=5-8).

(f) *Skn-1* KO mice exhibited increased energy expenditure compared with their WT littermates (n=9).

(g) qRT-PCR analysis revealed that the mitochondrial DNA content in skeletal muscle was significantly higher in *Skn-1* KO mice than in their WT littermates. The data are presented as the mean \pm SEM; **p<0.01, *p<0.05. See also Fig. S2.

Fig. 3. Metabolic Phenotypes of *Skn-1* KO Mice Fed a HFD

(a) Changes in body weight under HFD conditions. When fed a HFD for 12 weeks after 4 weeks of age, *Skn-1* KO mice exhibited dramatically reduced body weight compared with their WT littermates (n>54).

(b) *Skn-1* KO mice had a lower body fat percentage than their WT littermates, whereas there were no significant differences in muscle mass percentage between the two genotypes (n=18–26)

(c) *Skn-1* KO mice had lower tissue weights of epididymal and perirenal WAT (n=6–12).

(d) *Skn-1* KO and WT littermates had similar food intake at 8 weeks of age (n=8–10).

(e) *Skn-1* KO mice exhibited increased energy expenditure compared with their WT littermates (n=4). The data are presented as the mean \pm SEM; **p<0.01, *p<0.05. See also Fig. S3.

Fig. 4. Enhanced Catecholamine Secretion in *Skn-1* KO Mice Fed a HFD

(a) Serum triiodothyronine (T3), tetraiodothyronine (T4), and thyroid stimulating hormone (TSH) were comparable between *Skn-1* KO and WT littermates (n=7–8).

(b) Urinary epinephrine and dopamine were higher in *Skn-1* KO mice than their WT littermates (n=13–14). The data are presented as the mean \pm SEM; *p<0.05. See also Fig. S4.

Fig. 5. Reduced Insulin Secretion and Improved Glucose Tolerance and Insulin Resistance in *Skn-1* KO Mice

(a and b) Blood glucose (a) and plasma insulin (b) after glucose gavage (3.0 mg/g of body weight) when fed a normal chow diet. Blood glucose was comparable between *Skn-1* KO and WT littermates for 120 min after administration (n=21–33) (a). *Skn-1* KO mice exhibited a smaller increase in plasma insulin for 60 min after administration compared with their WT littermates (n=20-21) (b).

(c and d) Blood glucose (c) and plasma insulin (d) after glucose gavage (2.0 mg/g of body weight) of mice fed a HFD. Blood glucose was lower in *Skn-1* KO mice than their WT littermates for 120 min after administration (n=26–30) (c). Plasma insulin was lower in *Skn-1* KO mice than their WT littermates before glucose administration (p<0.05) and tended to be lower at 15 min after administration (p=0.10) (n=25–30) (d).

(e) Blood glucose after intraperitoneal administration of insulin (0.75 mU/g of body weight) when fed a HFD. *Skn-1* KO mice exhibited improved insulin resistance compared with WT littermates (n=5). The data are presented as the mean \pm SEM; **p<0.01, *p<0.05. See also Fig. S5.

Fig. 6. Schematic representation of the presumed metabolic pathways originating from brush cells and type II taste cells in the GI tract

Food components and digested nutrients are detected by the tongue and GI tract. In *Skn-1* KO mice, the lack of type II taste cells and brush cells results in increased catecholamine secretion. Lipolysis in WAT, serum levels of total ketone bodies, and thermogenesis in muscle are increased, whereas insulin secretion from the pancreas is reduced. Consequently, *Skn-1* KO mice have reduced body weight with lower body fat percentage due to higher energy expenditure.

References

- Andersen, B., Schonemann, M.D., Flynn, S.E., Pearse, R.V., 2nd, Singh, H., Rosenfeld, M.G. (1993). Skn-1a and Skn-1i: two functionally distinct Oct-2-related factors expressed in epidermis. *Science* 260, 78-82.
- Andersen, B., Weinberg, W.C., Rennekampff, O., McEvilly, R.J., Bermingham, J.R., Jr., Hooshmand, F., Vasilyev, V., Hansbrough, J.F., Pittelkow, M.R., Yuspa, S.H., Rosenfeld, M.G. (1997) Functions of the POU domain genes Skn-1a/i and Tst-1/Oct-6/SCIP in epidermal differentiation. *Genes Dev* 11, 1873-1884.
- Bahnsen, M., Burrin, J.M., Johnston, D.G., Pernet, A., Walker, M., and Alberti, K.G. (1984). Mechanisms of catecholamine effects on ketogenesis. *Am J Physiol* 247, E173-180.
- Barth, E., Albuszies, G., Baumgart, K., Matejovic, M., Wachter, U., Vogt, J., Radermacher, P., and Calzia, E. (2007). Glucose metabolism and catecholamines. *Crit Care Med* 35, S508-518.
- Bezencon, C., Furholz, A., Raymond, F., Mansourian, R., Metairon, S., Le Coutre, J., and Damak, S. (2008). Murine intestinal cells expressing Trpm5 are mostly brush cells and express markers of neuronal and inflammatory cells. *J Comp Neurol* 509, 514-525.
- Breitling, R., Armengaud, P., Amtmann, A., and Herzyk, P. (2004). Rank products: a simple, yet powerful, new method to detect differentially regulated genes in replicated microarray experiments. *FEBS Lett* 573, 83-92.
- Brixel, L.R., Monteilh-Zoller, M.K., Ingenbrandt, C.S., Fleig, A., Penner, R., Enklaar, T., Zabel, B.U., and Prawitt, D. (2010). TRPM5 regulates glucose-stimulated insulin secretion. *Pflugers Arch* 460, 69-76.
- Colsoul, B., Schraenen, A., Lemaire, K., Quintens, R., Van Lommel, L., Segal, A.,

- Owsianik, G., Talavera, K., Voets, T., Margolskee, R.F., Kokrashvili, Z., Gilon, P., Nilius, B., Schuit, F.C., and Vennekens, R. (2010). Loss of high-frequency glucose-induced Ca²⁺ oscillations in pancreatic islets correlates with impaired glucose tolerance in Trpm5^{-/-} mice. *Proc Natl Acad Sci U S A* 107, 5208-5213.
- Cummings, D.E., and Overduin, J. (2007). Gastrointestinal regulation of food intake. *J Clin Invest* 117, 13-23.
- Folch, J., Lees, M., and Sloane Stanley, G.H. (1957). A simple method for the isolation and purification of total lipides from animal tissues. *J Biol Chem* 226, 497-509.
- Furness, J.B. (2012). The enteric nervous system and neurogastroenterology. *Nat Rev Gastroenterol Hepatol* 9, 286-294.
- Gentleman, R.C., Carey, V.J., Bates, D.M., Bolstad, B., Dettling, M., Dudoit, S., Ellis, B., Gautier, L., Ge, Y., Gentry, J., Hornik, K., Hothorn, T., Huber, W., Iacus, S., Irizarry, R., Leisch, F., Li, C., Maechler, M., Rossini, A.J., Sawitzki, G., Smith, C., Smyth, G., Tierney, L., Yang, J.Y., and Zhang, J. (2004). Bioconductor: open software development for computational biology and bioinformatics. *Genome Biol* 5, R80.
- Gerbe, F., Brulin, B., Makrini, L., Legraverend, C., and Jay, P. (2009). DCAMKL-1 expression identifies Tuft cells rather than stem cells in the adult mouse intestinal epithelium. *Gastroenterology* 137, 2179-2180; author reply 2180-2171.
- Gerbe, F., Legraverend, C., and Jay, P. (2012). The intestinal epithelium tuft cells: specification and function. *Cell Mol Life Sci* 69, 2907-2917.
- Gerbe, F., van Es, J.H., Makrini, L., Brulin, B., Mellitzer, G., Robine, S., Romagnolo, B., Shroyer, N.F., Bourgaux, J.F., Pignodel, C., Clevers, H., and Jay, P. (2011). Distinct ATOH1 and Neurog3 requirements define tuft cells as a new secretory cell type in the intestinal epithelium. *J Cell Biol* 192, 767-780.

- Hochreiter, S., Clevert, D.A., and Obermayer, K. (2006) A new summarization method for Affymetrix probe level data. *Bioinformatics*. 22, 943-949.
- Ishimaru, Y., Inada, H., Kubota, M., Zhuang, H., Tominaga, M., and Matsunami, H. (2006). Transient receptor potential family members PKD1L3 and PKD2L1 form a candidate sour taste receptor. *Proc Natl Acad Sci U S A* 103, 12569-12574.
- Ishimaru, Y., Okada, S., Naito, H., Nagai, T., Yasuoka, A., Matsumoto, I., and Abe, K. (2005). Two families of candidate taste receptors in fishes. *Mech Dev* 122, 1310-1321.
- Jang, H.J., Kokrashvili, Z., Theodorakis, M.J., Carlson, O.D., Kim, B.J., Zhou, J., Kim, H.H., Xu, X., Chan, S.L., Juhaszova, M., Bernier, M., Mosinger, B., Margolskee, R.F., Egan, J.M. (2007). Gut-expressed gustducin and taste receptors regulate secretion of glucagon-like peptide-1. *Proc Natl Acad Sci U S A* 104, 15069-15074.
- Janssen, S., Laermans, J., Verhulst, P.J., Thijs, T., Tack, J., and Depoortere, I. (2011). Bitter taste receptors and alpha-gustducin regulate the secretion of ghrelin with functional effects on food intake and gastric emptying. *Proc Natl Acad Sci U S A* 108, 2094-2099.
- Katsurada, K., Maejima, Y., Nakata, M., Kodaira, M., Suyama, S., Iwasaki, Y., Kario, K., and Yada, T. (2014). Endogenous GLP-1 acts on paraventricular nucleus to suppress feeding: projection from nucleus tractus solitarius and activation of corticotropin-releasing hormone, nesfatin-1 and oxytocin neurons. *Biochem Biophys Res Commun* 451, 276-281.
- Kinzig, K.P., D'Alessio, D.A., and Seeley, R.J. (2002). The diverse roles of specific GLP-1 receptors in the control of food intake and the response to visceral illness. *J Neurosci* 22, 10470-10476.
- Larsson, M.H., Hakansson, P., Jansen, F.P., Magnell, K., and Brodin, P. (2015). Ablation

of TRPM5 in Mice Results in Reduced Body Weight Gain and Improved Glucose Tolerance and Protects from Excessive Consumption of Sweet Palatable Food when Fed High Caloric Diets. *PLoS One* 10, e0138373.

Lenders, J.W., Duh, Q.Y., Eisenhofer, G., Gimenez-Roqueplo, A.P., Grebe, S.K., Murad, M.H., Naruse, M., Pacak, K., and Young, W.F. Jr. (2014). Pheochromocytoma and paraganglioma: an endocrine society clinical practice guideline. *J Clin Endocrinol Metab* 99, 1915-1942.

Liman, E.R. (2010). A TRP channel contributes to insulin secretion by pancreatic beta-cells. *Islets* 2, 331-333.

Livak, K.J., and Schmittgen, T.D. (2001). Analysis of relative gene expression data using real-time quantitative PCR and the 2⁻(Delta Delta C(T)) Method. *Methods* 25, 402-408.

Markou, A., Sertedaki, A., Kaltsas, G., Androulakis, I., Marakaki, C., Pappa, T., Gouli, A., Papanastasiou, L., Fountoulakis, S., Zacharoulis, A., Karavidas, A., Ragkou, D., Charmandari, E., Chrousos, G.P., and Padiotis, G.P. (2015) Stress-induced Aldosterone Hyper-Secretion in a Substantial Subset of Patients With Essential Hypertension. *J Clin Endocrinol Metab* 100, 2857-2864.

Matsumoto, I., Ohmoto, M., Narukawa, M., Yoshihara, Y., and Abe, K. (2011). *Skn-1a* (*Pou2f3*) specifies taste receptor cell lineage. *Nat Neurosci* 14, 685-687.

Miura, S., Kawanaka, K., Kai, Y., Tamura, M., Goto, M., Shiuchi, T., Minokoshi, Y., Ezaki, O. (2007). An increase in murine skeletal muscle peroxisome proliferator-activated receptor-gamma coactivator-1alpha (*PGC-1alpha*) mRNA in response to exercise is mediated by beta-adrenergic receptor activation. *Endocrinology* 148, 3441-3448.

Moreira-Rodrigues, M., Quelhas-Santos, J., Roncon-Albuquerque, R., Serrao, P., Leite-Moreira, A., Sampaio-Maia, B., and Pestana, M. (2012). Blunted renal

dopaminergic system in a mouse model of diet-induced obesity. *Exp Biol Med* (Maywood) 237, 949-955.

Nakagawa, Y., Nagasawa, M., Yamada, S., Hara, A., Mogami, H., Nikolaev, V.O., Lohse, M.J., Shigemura, N., Ninomiya, Y., and Kojima, I. (2009). Sweet taste receptor expressed in pancreatic beta-cells activates the calcium and cyclic AMP signaling systems and stimulates insulin secretion. *PLoS One* 4, e5106.

Nakai, Y., Hashida, H., Kadota, K., Minami, M., Shimizu, K., Matsumoto, I., Kato, H., and Abe, K. (2008). Up-regulation of genes related to the ubiquitin-proteasome system in the brown adipose tissue of 24-h-fasted rats. *Biosci Biotechnol Biochem* 72, 139-148.

Nielsen, T.S., Jessen, N., Jorgensen, J.O., Moller, N., and Lund, S. (2014). Dissecting adipose tissue lipolysis: molecular regulation and implications for metabolic disease. *J Mol Endocrinol* 52, R199-222.

Ohmoto, M., Yamaguchi, T., Yamashita, J., Bachmanov, A.A., Hirota, J., and Matsumoto, I. (2013). *Pou2f3/Skn-1a* is necessary for the generation or differentiation of solitary chemosensory cells in the anterior nasal cavity. *Biosci Biotechnol Biochem* 77, 2154-2156.

Oya, M., Suzuki, H., Watanabe, Y., Sato, M., and Tsuboi, T. (2011). Amino acid taste receptor regulates insulin secretion in pancreatic beta-cell line MIN6 cells. *Genes Cells* 16, 608-616.

Prawitt, D., Monteilh-Zoller, M.K., Brixel, L., Spangenberg, C., Zabel, B., Fleig, A., and Penner, R. (2003). TRPM5 is a transient Ca^{2+} -activated cation channel responding to rapid changes in $[Ca^{2+}]_i$. *Proc Natl Acad Sci U S A* 100, 15166-15171.

Rindi, G., Leiter, A.B., Kopin, A.S., Bordi, C., and Solcia, E. (2004). The "normal" endocrine cell of the gut: changing concepts and new evidences. *Ann N Y Acad Sci* 1014,

1-12.

Rosengren, A.H., Jokubka, R., Tojjar, D., Granhall, C., Hansson, O., Li, D.Q., Nagaraj, V., Reinbothe, T.M., Tuncel, J., Eliasson, L., Groop, L., Rorsman, P., Salehi, A., Lyssenko, V., Luthman, H., and Renstrom, E. (2009). Overexpression of alpha2A-adrenergic receptors contributes to type 2 diabetes. *Science* 327, 217-220.

Saqui-Salces, M., Keeley, T.M., Grosse, A.S., Qiao, X.T., El-Zaatari, M., Gumucio, D.L., Samuelson, L.C., and Merchant, J.L. (2011). Gastric tuft cells express DCLK1 and are expanded in hyperplasia. *Histochem Cell Biol* 136, 191-204.

Schütz, B., Jurastow, I., Bader, S., Ringer, C., von Engelhardt, J., Chubanov, V., Gudermann, T., Diener, M., Kummer, W., Krasteva-Christ, G., and Weihe, E. (2015). Chemical coding and chemosensory properties of cholinergic brush cells in the mouse gastrointestinal and biliary tract. *Front Physiol.* 6, 87.

Simon, B.R., Learman, B.S., Parlee, S.D., Scheller, E.L., Mori, H., Cawthorn, W.P., Ning, X., Krishnan, V., Ma, Y.L., Tyrberg, B., and MacDougald, O.A. (2014) Sweet taste receptor deficient mice have decreased adiposity and increased bone mass. *PLoS One* 9, e86454.

Steiner, K.E., Stevenson, R.W., Adkins-Marshall, B.A., and Cherrington, A.D. (1991). The effects of epinephrine on ketogenesis in the dog after a prolonged fast. *Metabolism* 40, 1057-1062.

Strahler, J., Rohleder, N., and Wolf, J.M. (2015). Acute psychosocial stress induces differential short-term changes in catecholamine sensitivity of stimulated inflammatory cytokine production. *Brain Behav Immun* 43, 139-148.

Team, R.D.C., and Computing, R.F.f.S. (2005). R: A language and environment for statistical computing (Vienna, Austria)

Tschop, M.H., Speakman, J.R., Arch, J.R., Auwerx, J., Bruning, J.C., Chan, L., Eckel, R.H., Farese, R.V., Jr., Galgani, J.E., Hambly, C., Herman, M.A., Horvath, T.L., Kahn, B.B., Kozma, S.C., Maratos-Flier, E., Muller, T.D., Munzberg, H., Pfluger, P.T., Plum, L., Reitman, M.L., Rahmouni, K., Shulman, G.I., Thomas, G., Kahn, C.R., and Ravussin, E. (2011). A guide to analysis of mouse energy metabolism. *Nat Methods* 9, 57-63.

Tsunoda, M., Aoyama, C., Ota, S., Tamura, T., and Funatsu, T. (2011). Extraction of catecholamines from urine using a monolithic silica disk-packed spin column and high-performance liquid chromatography-electrochemical detection. *Anal Methods-Uk* 3, 582-585.

Vahl, T.P., Tauchi, M., Durler, T.S., Elfers, E.E., Fernandes, T.M., Bitner, R.D., Ellis, K.S., Woods, S.C., Seeley, R.J., Herman, J.P., and D'Alessio, D.A. (2007). Glucagon-like peptide-1 (GLP-1) receptors expressed on nerve terminals in the portal vein mediate the effects of endogenous GLP-1 on glucose tolerance in rats. *Endocrinology* 148, 4965-4973.

van der Flier, L.G., and Clevers, H. (2009). Stem cells, self-renewal, and differentiation in the intestinal epithelium. *Annu Rev Physiol* 71, 241-260.

Watanabe, N., Inagawa, K., Shibata, M., and Osakabe, N. (2014). Flavan-3-ol fraction from cocoa powder promotes mitochondrial biogenesis in skeletal muscle in mice. *Lipids Health Dis* 13, 64.

Watanabe, T., Kawada, T., Kurosawa, M., Sato, A., and Iwai, K. (1988). Adrenal sympathetic efferent nerve and catecholamine secretion excitation caused by capsaicin in rats. *Am J Physiol* 255, E23-27.

Wu, T., Rayner, C.K., and Horowitz, M. (2015). Incretins. *Handb Exp Pharmacol*.

Yamaguchi, T., Yamashita, J., Ohmoto, M., Aoude, I., Ogura, T., Luo, W., Bachmanov,

A.A., Lin, W., Matsumoto, I., and Hirota, J. (2014). Skn-1a/Pou2f3 is required for the generation of Trpm5-expressing microvillous cells in the mouse main olfactory epithelium. *BMC Neurosci* 15, 13.

Yamamoto, K., and Ishimaru, Y. (2013). Oral and extra-oral taste perception. *Semin Cell Dev Biol* 24, 240-246.

Yarmolinsky D.A., Zuker, C.S., and Ryba, N.J. (2009). Common sense about taste: from mammals to insects. *Cell* 139, 234-244.

Young, R.L. (2011). Sensing via intestinal sweet taste pathways. *Front Neurosci* 5, 23.

Yukawa, K., Yasui, T., Yamamoto, A., Shiku, H., Kishimoto, T., and Kikutani, H. (1993).

Epoc-1: a POU-domain gene expressed in murine epidermal basal cells and thymic stromal cells. *Gene* 133, 163-169.

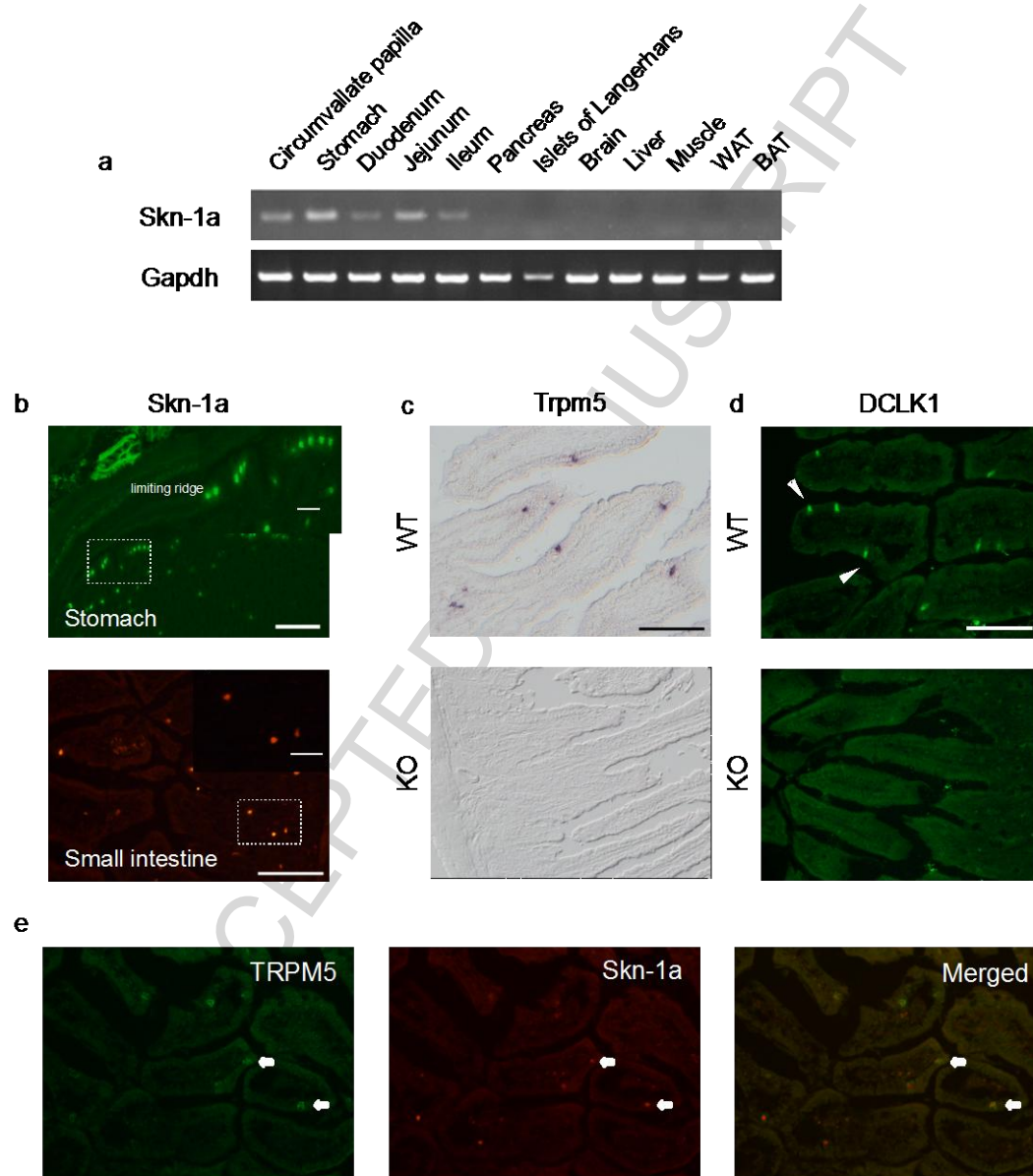


Figure 1 Ushima et al.

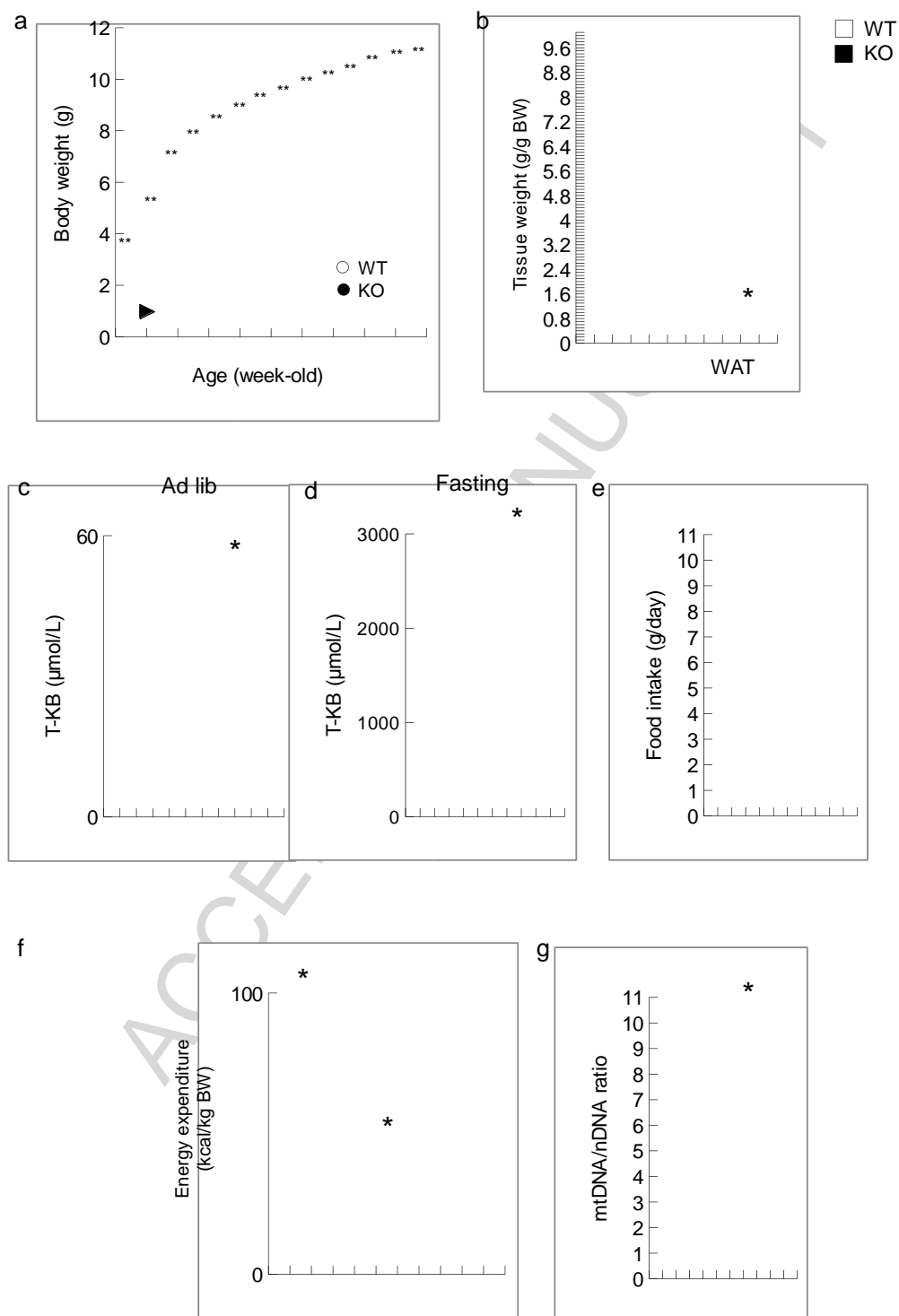


Figure 2 Ushima et al.

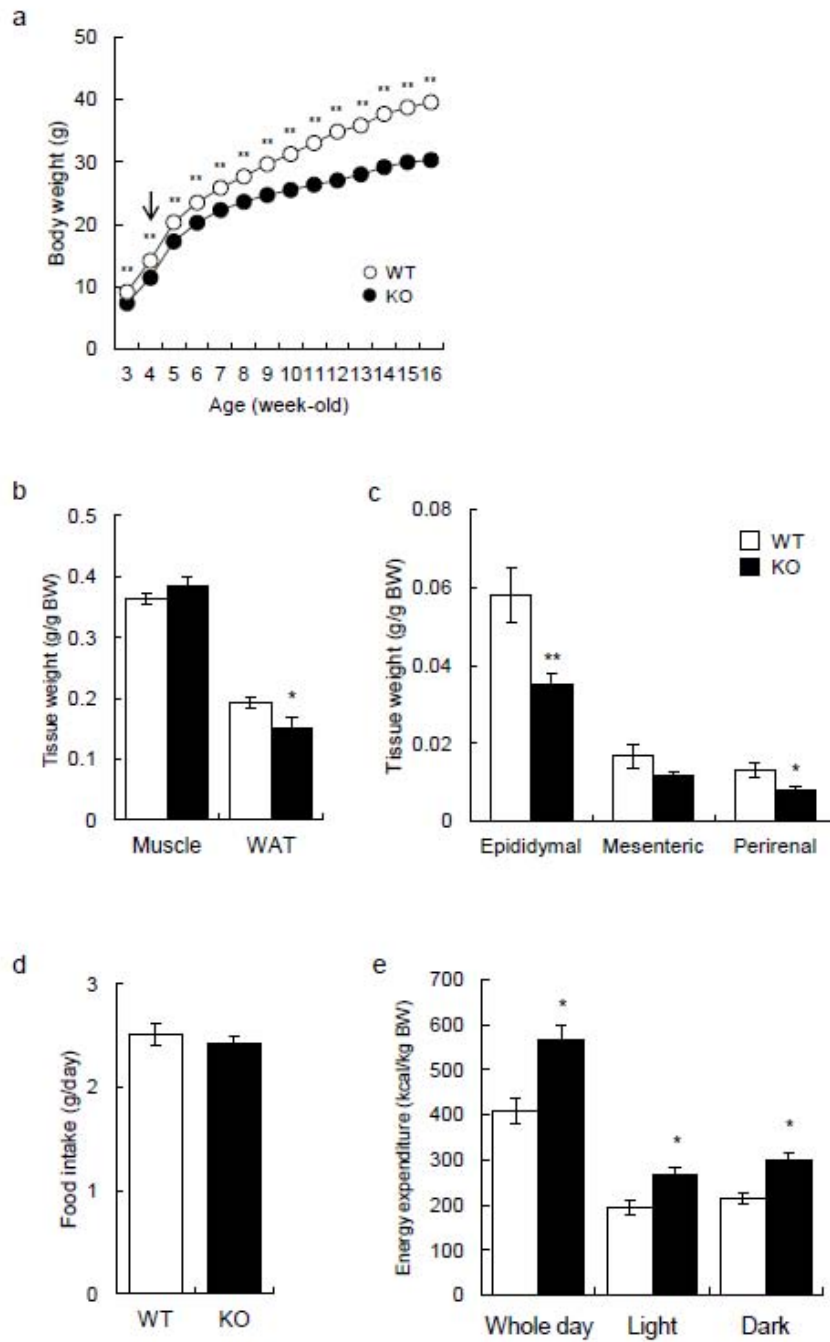


Figure 3 Ushiyama et al.

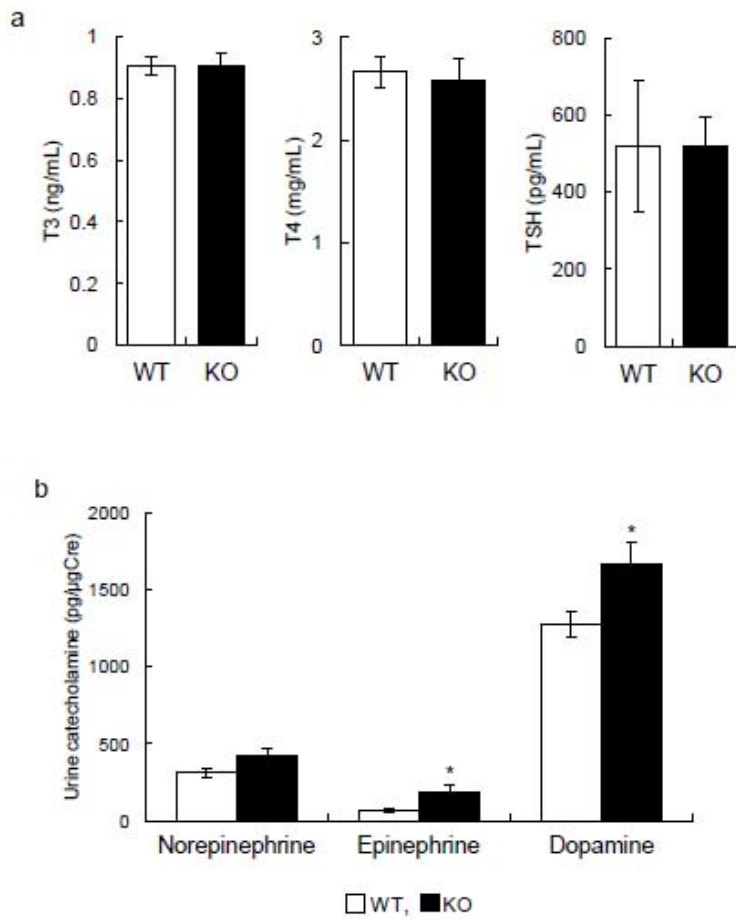


Figure 4 Ushiyama et al.

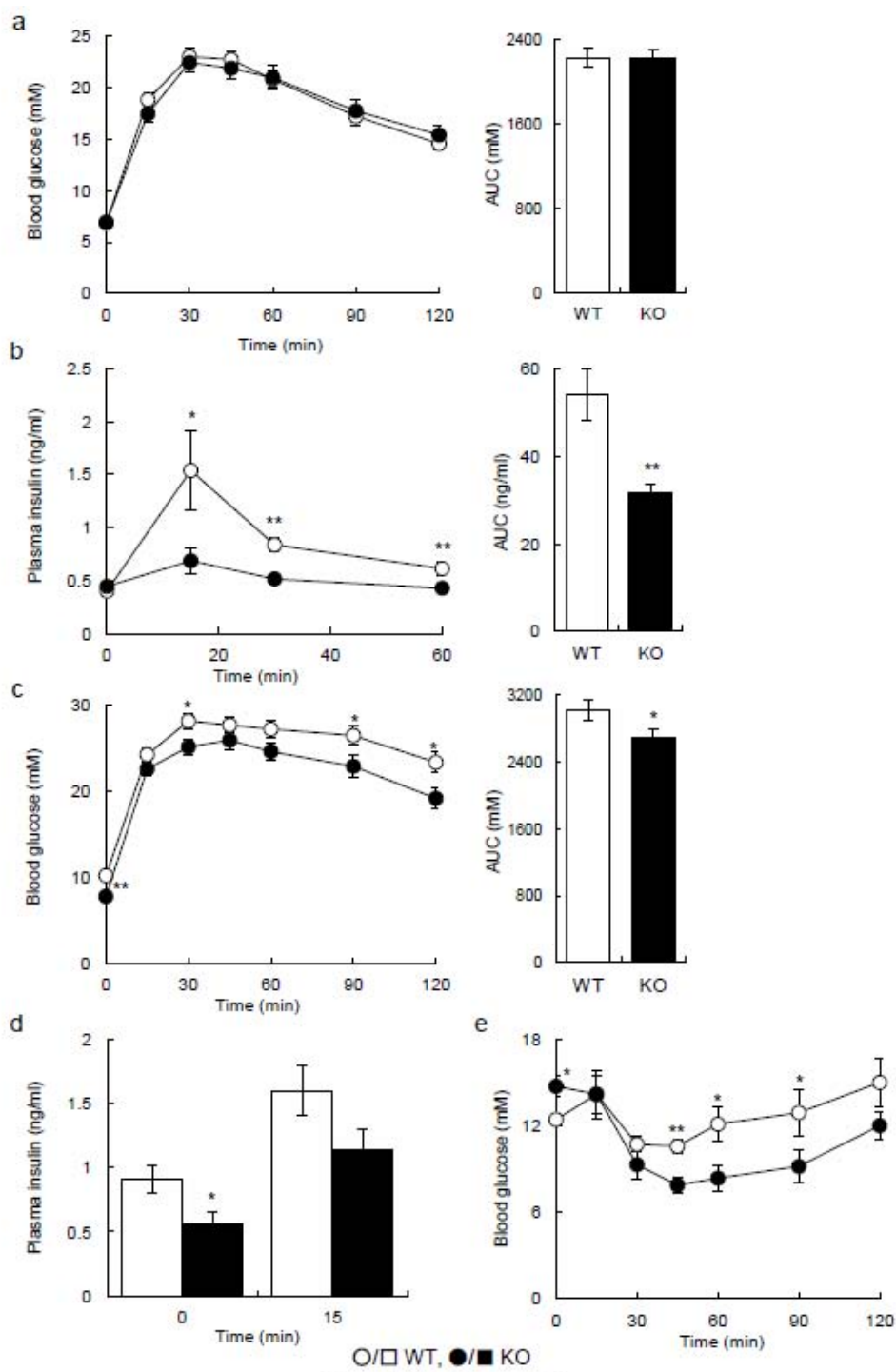


Figure 5 Ushima et al.

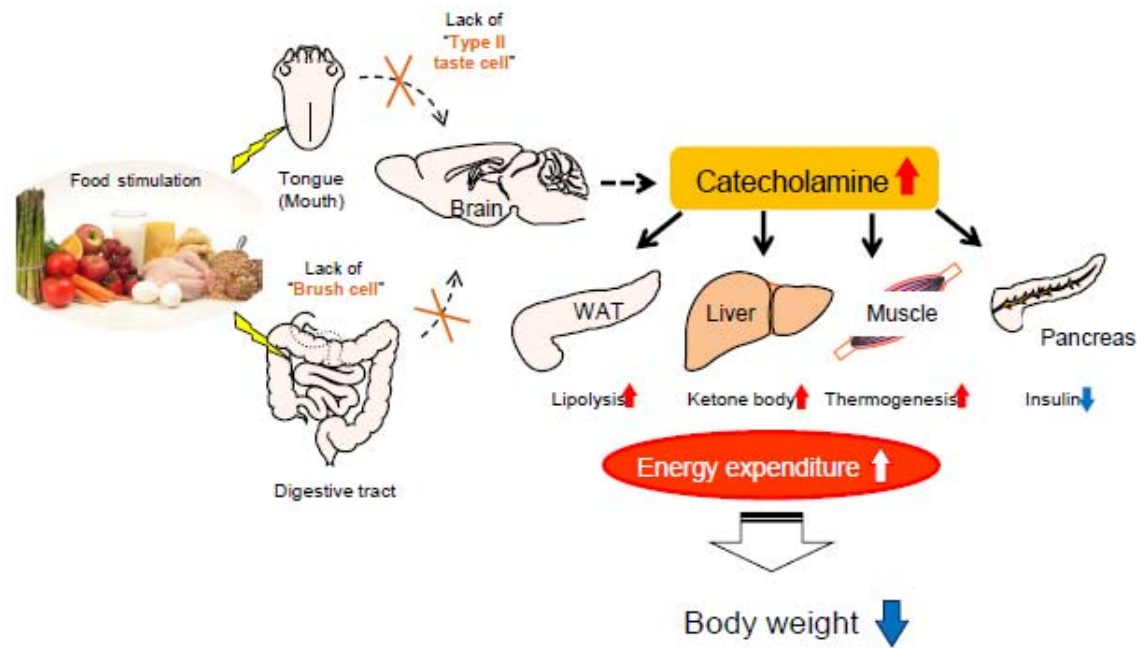


Figure 6 Ushiyama et al.

Table 1 Up-regulation genes related to mitochondrial function
in skeletal muscle

Gene Symbol	Gene Name	Probe ID
ABCD2	ATP-binding cassette, sub-family D (ALD), member 2	1419748_at
Ociad2	OCIA domain containing 2	1435917_at
Pptc7	PTC7 protein phosphatase homolog (S. cerevisiae)	1455958_s_at
4930402E16Rik	RIKEN cDNA4930402E16Rik gene	1459869_x_at
8430408G22Rik	RIKEN cDNA 8430408G22 gene	1433837_at
Tbc1d15	TBC1 domain family, member 15	1416062_at
Xaf1	XIAP associated factor 1	1443698_at
Col4a3bp	collagen, type IV, alpha 3 (Goodpasture antigen) binding protein	1420384_at
Dsp	desmoplakin	1435493_at, 1435494_s_at
DlaT	dihydrolipoamide S-acetyltransferase (E2 component of pyruvate dehydrogenase complex)	1426264_at, 1426265_x_at

Fdx1	ferredoxin 1	1449108_at
Gpam	glycerol-3-phosphate acyltransferase, mitochondrial	1419499_at
Hk2	hexokinase 2	1422612_at
Coq10b	coenzyme Q10 homolog B (S. cerevisiae)	1460510_a_at
Immt	inner membrane protein, mitochondrial	1429533_at
Ide	insulin degrading enzyme	1423121_at, 1435140_at
Krt5	keratin 5	1424096_at
Kif1b	kinesin family member 1B	1423995_at, 1451642_at, 1451200_at, 1425270_at
Elov16	ELOVL family member 6, elongation of long chain fatty acids (yeast)	1417403_at
Csde1	cold shock domain containing E1, RNA binding	1423997_at
Prkca	protein kinase C, alpha	1437393_at, 1446598_at, 1450945_at
Ppm1k	protein phosphatase 1K (PP2C domain containing)	1441988_at
Ppp3ca	protein phosphatase 3, catalytic subunit,	1426401_at, 1438478_a_at

	alpha isoform	
Reep1	receptor accessory protein 1	1433509_s_at
ND5	NADH dehydrogenase subunit 5	1426088_at
Opa1	optic atrophy 1	1434890_at
Slc25a12	solute carrier family 25 (mitochondrial carrier, Aralar), member 12	1436440_at
Slc25a25	solute carrier family 25 (mitochondrial carrier, phosphate carrier), member 25	1424735_at, 1447856_x_at
Tmtc1	transmembrane and tetratricopeptide repeat containing 1	1435261_at
Tap1	transporter 1, ATP-binding cassette, sub-family B (MDR/TAP)	1416016_at
Ucp3	uncoupling protein 3 (mitochondrial, proton carrier)	1420658_at